

Buckling response with stretching effect of carbon nanotube-reinforced composite beams resting on elastic foundation

Zoubida Khelifa^{*1,2}, Lazreg Hadji^{1,3}, Tahar Hassaine Daouadji^{1,3} and Mohamed Bourada²

¹Department of Civil Engineering, Ibn Khaldoun University, BP 78 Zaaroura, Tiaret (14000), Algeria

²Department of Civil Engineering, Material and Hydrology Laboratory, University of Sidi Bel Abbes, Faculty of Technology, Algeria

³Laboratory of Geomatics and Sustainable Development, Ibn Khaldoun University of Tiaret, Algeria

(Received December 28, 2017, Revised April 15, 2018, Accepted April 30, 2018)

Abstract. This study deals with buckling analysis with stretching effect of functionally graded carbon nanotube-reinforced composite beams resting on an elastic foundation. The single-walled carbon nanotubes (SWCNTs) are aligned and distributed in polymeric matrix with different patterns of reinforcement. The material properties of the CNTRC beams are estimated by using the rule of mixture. The significant feature of this model is that, in addition to including the shear deformation effect and stretching effect it deals with only 4 unknowns without including a shear correction factor. The equilibrium equations have been obtained using the principle of virtual displacements. The mathematical models provided in this paper are numerically validated by comparison with some available results. New results of buckling analyses of CNTRC beams based on the present theory with stretching effect is presented and discussed in details. the effects of different parameters of the beam on the buckling responses of CNTRC beam are discussed.

Keywords: buckling; stretching effect; CNTRC beams; elastic foundation

1. Introduction

Due to their exceptional mechanical, thermal and electrical properties, carbon nanotubes (CNTs) are considered as one of the most promising reinforcement materials for high performance structural and multifunctional composites with tremendous application potentials (Rafiee *et al.* (2012)) and have taken a considerable research interests in the materials engineering community (Tounsi *et al.* 2013a). Compared with the classical carbon fiber-reinforced polymer composites, carbon nanotube-reinforced composites (CNTRCs) have the potential of improving increased strength and stiffness. In the last few years a lot of research has been performed on composite structure reinforcement by nanotubes. Most of this research relates to carbon nanotubes and composite structure properties. A review and comparisons of the mechanical properties of single- and multi-walled carbon nanotube reinforced composites fabricated by various processes are given by Coleman *et al.* (2006), in which the composites based on chemically modified nanotubes show the best results since functionalization should significantly enhance both dispersion and stress transfer. From then, many researchers studied the material characteristics of CNTRCs (Hu *et al.* 2005, Zhu *et al.* 2007). Rafiee *et al.* (2013) studied the thermal bifurcation buckling of piezoelectric carbon nanotube reinforced composite beams. Ray and Batra (2007) presented a new carbon CNT-reinforced 1-3 piezoelectric composite for the active control

of smart structures. Based on Timoshenko beam theory, Ke *et al.* (2013) studied the dynamic stability response of functionally graded (FG) nanocomposite beams reinforced by SWCNTs. Lei *et al.* (2013) presented a large deflection analysis of FG-CNT reinforced composite plates by considering different boundary conditions. Hajnayeb and Khadem (2015) developed an analytical study on the nonlinear vibration of a doublewalled carbon nanotube. Rafiee *et al.* (2017) presented the dynamics, vibration and control of rotating composite beams and blades: A critical review. Berrabah *et al.* (2013) studied the comparison of various refined nonlocal beam theories for bending, vibration and buckling analysis of nanobeams. Recently, Yas and Samadi (2012) analyze the free vibrations and buckling analysis of carbon nanotube-reinforced composite Timoshenko beams on elastic foundation. Wattanasakulpong and Ungbhakorn (2013) studied the Analytical solutions for bending, buckling and vibration responses of carbon nanotube-reinforced composite beams resting on elastic foundation. Barzoki *et al.* (2013) analyze the temperature-dependent nonlocal nonlinear buckling of functionally graded SWCNT-reinforced microplates embedded in an orthotropic elastomeric medium. Mareishi *et al.* (2014) investigated the nonlinear free vibration, postbuckling and nonlinear static deflection of piezoelectric fiber-reinforced laminated composite beams. Rafiee *et al.* (2014) studied the non-linear dynamic stability of piezoelectric functionally graded carbon nanotube-reinforced composite plates with initial geometric imperfection. Bourada *et al.* (2015) used a new simple shear and normal deformations theory for functionally graded beams. Hamidi *et al.* (2015) proposed a sinusoidal plate theory with 5-unknowns and stretching effect for

*Corresponding author, Ph.D.
E-mail: ZouKhe87@yahoo.com

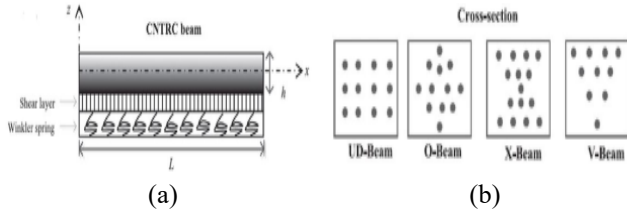


Fig. 1(a) Geometry of a CNTRC beam on elastic foundation ; and (b) cross sections of different patterns of reinforcement

thermomechanical bending of functionally graded sandwich plates. Draiche *et al.* (2016) used a refined theory with stretching effect for the flexure analysis of laminated composite plates. Tagrara *et al.* (2015) studied the bending, buckling and vibration responses of functionally graded carbon nanotube-reinforced composite beams. As far as we know, there has been no investigation on buckling with stretching effect of carbon nanotube-reinforced composite beams resting on elastic foundation. Rafiee *et al.* (2015) developed the nonlinear Response of Piezoelectric Nanocomposite Plates: Large Deflection, Post-Buckling and Large Amplitude Vibration. He *et al.* (2015) presented the nonlinear dynamics of piezoelectric nanocomposite energy harvesters under parametric resonance.

In the present study, the buckling of the CNTRC beams with stretching effect is investigated using the Navier solution method. The simply supported CNTRC beams which are placed on the Pasternak elastic foundation, including a shear layer and Winkler spring, are considered. New solutions of buckling loads based on the present refined shear deformation theory with stretching effect are presented and discussed in details. Several aspects of spring constants, thickness ratios, stretching effect, CNT volume fractions, types of CNT distribution, etc., which have considerable impact on the analytical solutions, are also investigated.

2. CNTRC beams

A straight CNTRC beam made from a mixture of SWCNT and anisotropic polymer matrix is considered. The beam, having length (L) and thickness (h), is placed on the Pasternak elastic foundation, including a shear layer and Winkler spring, as shown in Fig. 1(a). In this study, the beams are assumed to have four different patterns of reinforcement over the cross sections as shown in Fig. 1(b).

The material properties of CNTRC beams can be computed utilizing the rule of mixture which gives the effective Young's modulus and shear modulus of CNTRC beams as (Shen *et al.* 2009, Bakhti *et al.* 2013, Kaci *et al.* 2012, Wattanasakulpong and Ungbhakorn 2013).

$$E_{11} = \eta_1 V_{cnt} E_{11}^{cnt} + V_p E_p \quad (1a)$$

$$\frac{\eta_2}{E_{22}} = \frac{V_{cnt}}{E_{22}^{cnt}} + \frac{V_p}{E_p} \quad (1b)$$

$$\frac{\eta_3}{G_{22}} = \frac{V_{cnt}}{G_{12}^{cnt}} + \frac{V_p}{E_p} \quad (1c)$$

where E_{11}^{cnt} ; E_{22}^{cnt} and G_{12}^{cnt} are the Young's modulus and shear modulus of SWCNT, respectively and E_p and G_p are the corresponding material properties of the polymer matrix. Also, V_{cnt} and V_p are the volume fractions for carbon nanotube and the polymer matrix, respectively, with the relation of $V_{cnt} + V_p = 1$. To introduce the size-dependent material properties of SWCNT, the CNT efficiency parameters, η_i ($i=1, 2, 3$), are considered. They can be obtained from matching the elastic moduli of CNTRCs estimated by the MD simulation with the numerical results determined by the rule of mixture (Han and Elliott 2007). By employing the same rule, Poisson's ratio (ν) and mass density (ρ) of the CNTRC beams are expressed as

$$\nu = V_{cnt} \nu^{cnt} + V_p \nu^p, \quad \rho = V_{cnt} \rho^{cnt} + V_p \rho^p \quad (2)$$

where ν^{cnt} , ν^p and ρ^{cnt} , ρ^p are the Poisson's ratios and densities of the CNT and polymer matrix respectively. For different patterns of carbon nanotube reinforcement distributed within the cross sections of the beams as shown in Fig. 1(b), the continuous mathematical functions employing for introducing the distributions of material constituents are expressed below

UD-Beam

$$V_{cnt} = V_{cnt}^* \quad (3a)$$

O-Beam

$$V_{cnt} = 2 \left(1 - 2 \frac{|z|}{h} \right) V_{cnt}^* \quad (3b)$$

X-Beam

$$V_{cnt} = 4 \frac{|z|}{h} V_{cnt}^* \quad (3c)$$

where V_{cnt}^* is the considered volume fraction of CNTs, which can be determined from the following equation

$$V_{cnt}^* = \frac{W_{cnt}}{W_{cnt} + (\rho^{cnt} / \rho^m)(1 - W_{cnt})} \quad (4)$$

where W_{cnt} is the mass fraction of CNTs. From Eq. (3), it can be seen that the O-, X- and V-Beams are some types of functionally graded beams in which their material constituents are varied continuously within their thicknesses; while, the UD-Beam has uniformly distributed CNT reinforcement. In this work, the CNT efficiency parameters (η_i) associated with the considered volume fraction V_{cnt}^* are : $\eta_1 = 1.2833$ and $\eta_2 = \eta_3 = 1.0556$ for the case of $V_{cnt}^* = 0.12$; $\eta_1 = 1.3414$ and $\eta_2 = \eta_3 = 1.7101$ for the case of

$V_{cnt}^* = 0.17$; $\eta_1 = 1.3228$ and $\eta_2 = \eta_3 = 1.7380$
for the case of $V_{cnt}^* = 0.28$ (Yas and Samadi 2012).

3. Theory and formulations

3.1 Kinematics and constitutive equations

Consider a shear deformation beam theory, the displacement field consisting of the axial displacement, u , and the transverse displacement, w , can be written in the following forms

$$u(x, z) = u_0(x) - z \frac{\partial w_b}{\partial x} - f(z) \frac{\partial w_s}{\partial x} \quad (5a)$$

$$w(x, z) = w_b(x) + w_s(x) + g(z)\varphi_z(x) \quad (5b)$$

where u_0 is the axial displacement, w_b and w_s are the bending and shear components of transverse displacement along the mid-plane of the beam. The additional displacement φ_z accounts for the effect of normal stress is included and $g(z)$ is given as follows

$$g(z) = 1 - f'(z) \quad (6a)$$

In this work, the shape function $f(z)$ is chosen based on a trigonometric function as (Tounsi *et al.* 2013)

$$f(z) = z - \frac{h}{\pi} \sin\left(\frac{\pi}{h} z\right) \quad (6b)$$

Clearly, the displacement field in Eq. (5) contains only four unknowns (u_0 , w_b , w_s , φ_z). The strains associated with the displacements in Eq. (5) are

$$\varepsilon_x = \frac{\partial u_0}{\partial x} - z \frac{\partial^2 w_b}{\partial x^2} - f(z) \frac{\partial^2 w_s}{\partial x^2} \quad (7a)$$

$$\varepsilon_z = g'(z)\varphi_z \quad (7b)$$

$$\gamma_{xz} = g(z) \left(\frac{\partial w_s}{\partial x} + \frac{\partial \varphi_z}{\partial x} \right) \quad (7c)$$

It can be seen from Eq. (7c) that the transverse shears strain γ_{xz} is equal to zero at the top ($z=h/2$) and bottom ($z=-h/2$) surfaces of the beam, thus satisfying the zero transverse shear stress conditions.

By assuming that the material of CNTRC beam obeys Hooke's law, the stresses in the beam become

$$\sigma_x = Q_{11}(z) \varepsilon_x + Q_{13}(z) \varepsilon_z \quad (8a)$$

$$\tau_{xz} = Q_{55}(z) \gamma_{xz} \quad (8b)$$

$$\sigma_z = Q_{13}(z) \varepsilon_x + Q_{33}(z) \varepsilon_z \quad (8c)$$

where

$$Q_{11}(z) = Q_{33}(z) = \frac{E_{11}(z)}{1 - \nu^2} \quad (8d)$$

$$Q_{13}(z) = \nu Q_{11}(z) \text{ and } Q_{55}(z) = G_{12}(z)$$

3.2 Governing equations

The governing equations of equilibrium can be derived by using the principle of virtual displacements. The principle of virtual work in the present case yields

$$\begin{aligned} & \int_{-h/2}^{h/2} [\sigma_x \delta \varepsilon_x + \sigma_z \delta \varepsilon_z + \tau_{xz} \delta \gamma_{xz}] dz dx \\ & + \int_0^L \left[K_w (w_b + w_s) \delta (w_b + w_s) - K_s \frac{\partial^2 (w_b + w_s)}{\partial x^2} \delta (w_b + w_s) \right] dx \\ & - \int_0^L \left[N_x^0 \frac{d(w_b + w_s + g\varphi_z)}{dx} \frac{d\delta(w_b + w_s + g\varphi_z)}{dx} \right] dx \end{aligned} \quad (9)$$

where K_w and K_s are the Winkler and shearing layer spring constants which can be determined from $K_w = \beta_w A_{110} / L^2$ and $K_s = \beta_s A_{110}$ in which β_w and β_s are the corresponding spring constant factors. It is also defined that A_{110} is the extension stiffness or the value of A_{11} of a homogeneous beam made of pure matrix material.

Substituting Eqs. (7) and (8) into Eq. (9) and integrating through the thickness of the beam, Eq. (9) can be rewritten as

$$\begin{aligned} & \int_0^L \left[N_x \delta \frac{\partial u_0}{\partial x} - M_x^b \delta \frac{\partial^2 w_b}{\partial x^2} - M_x^s \delta \frac{\partial^2 w_s}{\partial x^2} + R_z \delta \varphi_z + Q_{xz} \delta \left(\frac{\partial w_s}{\partial x} + \frac{\partial \varphi_z}{\partial x} \right) \right] dx \\ & + \int_0^L \left[K_w (w_b + w_s) \delta (w_b + w_s) - K_s \frac{\partial^2 (w_b + w_s)}{\partial x^2} \delta (w_b + w_s) \right] dx \\ & - \int_0^L \left[N_x^0 \frac{\partial (w_b + w_s + g\varphi_z)}{\partial x} \frac{\partial \delta (w_b + w_s + g\varphi_z)}{\partial x} \right] dx = 0 \end{aligned} \quad (10)$$

where N_x , M_x^b , M_x^s and Q_{xz} are the stress resultants defined by

$$(N_x, M_x^b, M_x^s) = \int_{-\frac{h}{2}}^{\frac{h}{2}} (1, z, f) \sigma_x dz \quad (11)$$

$$Q_{xz} = \int_{-\frac{h}{2}}^{\frac{h}{2}} g \tau_{xz} dz \text{ and } R_z = \int_{-\frac{h}{2}}^{\frac{h}{2}} \sigma_z g'(z) dz$$

The governing equations of equilibrium can be derived from Eq. (10) by integrating the displacement gradients by parts and setting the coefficients zero δu_0 , δw_b , δw_s , $\delta \varphi_z$. Thus, one can obtain the equilibrium equations associated with the present refined shear deformation theory

$$\delta u_0 : \frac{\partial N_x}{\partial x} = 0 \quad (12a)$$

$$\delta w_b : \frac{\partial^2 M_x^b}{\partial x^2} + N_x^0 \frac{\partial^2 (w_b + w_s + g\varphi_z)}{\partial x^2} + K_s \left(\frac{\partial^2 (w_b + w_s)}{\partial x^2} \right) - K_w (w_b + w_s) = 0 \quad (12b)$$

$$\delta w_s : \frac{\partial^2 M_x}{\partial x^2} + \frac{\partial Q_x}{\partial x} + N_x^0 \frac{\partial^2 (w_b + w_s + g\varphi_z)}{\partial x^2} + K_s \left(\frac{\partial^2 (w_b + w_s)}{\partial x^2} \right) - K_w (w_b + w_s) = 0 \quad (12c)$$

$$\delta \varphi_z : -R_z + \frac{\partial Q_x}{\partial x} + N_x^0 g \frac{\partial^2 (w_b + w_s + g\varphi_z)}{\partial x^2} = 0 \quad (12d)$$

Eqs. (12) can be expressed in terms of displacements (u_0, w_b, w_s, φ_z) by using Eqs. (5), (7), (8) and (11) as follows

$$A_{11} \frac{\partial^2 u_0}{\partial x^2} - B_{11} \frac{\partial^3 w_b}{\partial x^3} - B_{11}^s \frac{\partial^3 w_s}{\partial x^3} + X_{13} \frac{\partial \varphi_z}{\partial x} = 0 \quad (13a)$$

$$B_{11} \frac{\partial^3 u_0}{\partial x^3} - D_{11} \frac{\partial^4 w_b}{\partial x^4} - D_{11}^s \frac{\partial^4 w_s}{\partial x^4} + Y_{13} \frac{\partial^2 \varphi_z}{\partial x^2} + N_x^0 \frac{\partial^2 (w_b + w_s + g\varphi_z)}{\partial x^2} + K_s \left(\frac{\partial^2 (w_b + w_s)}{\partial x^2} \right) - K_w (w_b + w_s) = 0 \quad (13b)$$

$$B_{11} \frac{\partial^3 u_0}{\partial x^3} - D_{11} \frac{\partial^4 w_b}{\partial x^4} - H_{11} \frac{\partial^4 w_s}{\partial x^4} + A_{55} \frac{\partial^2 w_s}{\partial x^2} + (Y_{13}^s + A_{55}^s) \frac{\partial^2 \varphi_z}{\partial x^2} + q + K_s \left(\frac{\partial^2 (w_b + w_s)}{\partial x^2} \right) - K_w (w_b + w_s) = 0 \quad (13c)$$

$$-X_{13} \frac{\partial u_0}{\partial x} + Y_{13} \frac{\partial^2 w_b}{\partial x^2} + (Y_{13}^s + A_{55}^s) \frac{\partial^2 w_s}{\partial x^2} + A_{55}^s \frac{\partial^2 \varphi_z}{\partial x^2} - Z_{33} \varphi_z + N_x^0 g \frac{\partial^2 (w_b + w_s + g\varphi_z)}{\partial x^2} = 0 \quad (13d)$$

where A_{11}, D_{11} , etc., are the beam stiffness, defined by

$$A_{11} = \int_{-\frac{h}{2}}^{\frac{h}{2}} Q_{11} dz, \quad B_{11} = \int_{-\frac{h}{2}}^{\frac{h}{2}} Q_{11} z dz, \quad (14a)$$

$$B_{11}^s = \int_{-\frac{h}{2}}^{\frac{h}{2}} Q_{11} f dz, \quad X_{13} = \int_{-\frac{h}{2}}^{\frac{h}{2}} Q_{13} g' dz,$$

$$D_{11} = \int_{-\frac{h}{2}}^{\frac{h}{2}} Q_{11} z^2 dz, \quad D_{11}^s = \int_{-\frac{h}{2}}^{\frac{h}{2}} Q_{11} z f dz, \quad (14b)$$

$$Y_{13} = \int_{-\frac{h}{2}}^{\frac{h}{2}} Q_{13} z g' dz, \quad H_{11}^s = \int_{-\frac{h}{2}}^{\frac{h}{2}} Q_{11} f^2 dz,$$

$$Y_{13}^s = \int_{-\frac{h}{2}}^{\frac{h}{2}} Q_{13} f g' dz, \quad Z_{33} = \int_{-\frac{h}{2}}^{\frac{h}{2}} Q_{13} [g']^2 dz, \quad (14c)$$

$$A_{55}^s = \int_{-\frac{h}{2}}^{\frac{h}{2}} Q_{55} g^2 dz,$$

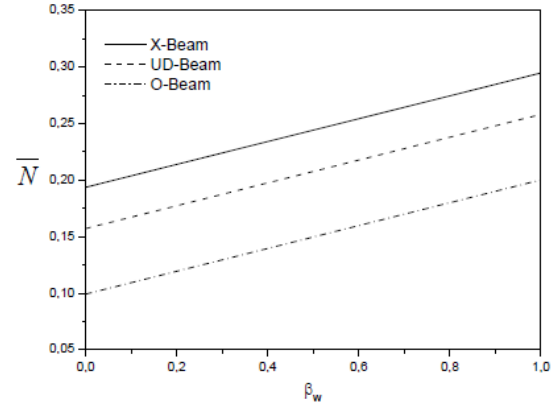


Fig. 2 Effect of Winkler modulus parameter on the critical buckling loads of CNTRC beams ($L/h=10$; $\beta_s=0$; $V_{cnt}^* = 0.12$)

4. Analytical solution

The equilibrium equations admit the Navier solutions for simply supported beams. The variables u_0, w_b, w_s, φ_z , can be written by assuming the following variations

$$\begin{Bmatrix} u_0 \\ w_b \\ w_s \\ \varphi_z \end{Bmatrix} = \sum_{m=1}^{\infty} \begin{Bmatrix} U_m \cos(\lambda x) \\ w_{bm} \sin(\lambda x) \\ w_{sm} \sin(\lambda x) \\ \phi_{zm} \sin(\lambda x) \end{Bmatrix} \quad (15)$$

where U_m, W_{bm}, W_{sm} and φ_{zm} are arbitrary parameters to be determined, and $\lambda = m\pi/L$.

Substituting the expressions of u_0, w_b, w_s, φ_z and from Eqs. (15) into the equilibrium equations of Eq. (13), the analytical solutions can be obtained from the following equations

$$([K] - [N])\{\Delta\} = \{0\} \quad (16)$$

where

$$[K] = \begin{bmatrix} a_{11} & a_{12} & a_{13} & a_{14} \\ a_{12} & a_{22} & a_{23} & a_{24} \\ a_{13} & a_{23} & a_{33} & a_{34} \\ a_{14} & a_{24} & a_{34} & a_{44} \end{bmatrix}; \quad [N] = \begin{bmatrix} 0 & 0 & 0 & 0 \\ 0 & k & k & k \\ 0 & k & k & k \\ 0 & k & k & k \end{bmatrix}; \quad \{\Delta\} = \begin{Bmatrix} U_m \\ W_{bm} \\ W_{sm} \\ \phi_{zm} \end{Bmatrix} \quad (17)$$

Where

$$\begin{aligned} a_{11} &= A_{11} \lambda^2, a_{12} = -B_{11} \lambda^3, a_{13} = -B_{11}^s \lambda^3, a_{14} = -X_{13} \lambda, a_{22} = D_{11} \lambda^4 + K_w + K_s \lambda^2, \\ a_{23} &= D_{11}^s \lambda^4 + K_w + K_s \lambda^2, a_{24} = Y_{13} \lambda^2, a_{33} = H_{11}^s \lambda^4 + A_{55}^s \lambda^2 + K_w + K_s \lambda^2, \\ a_{34} &= Y_{13}^s \lambda^2 + A_{55}^s \lambda^2, a_{44} = A_{55}^s \lambda^2 + Z_{33}, k = N_x^0 \lambda^2 \end{aligned} \quad (18)$$

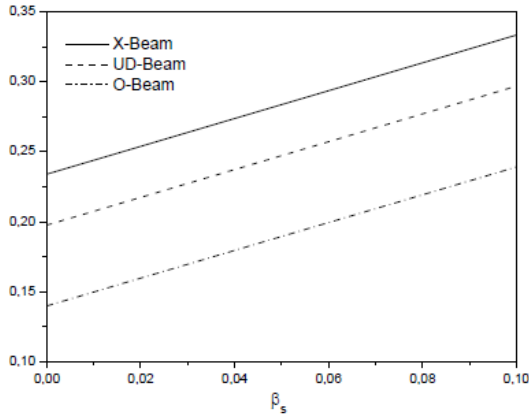


Fig. 3 Effect of Pasternak shear modulus parameter the critical buckling loads of CNTRC beams ($L/h=10$; $\beta_w=0.4$; $V_{cnt}^* = 0.12$)

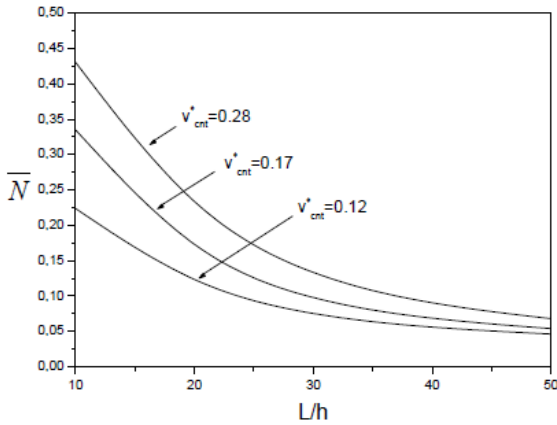


Fig. 4 Dimensionless critical buckling loads of X Beam on elastic foundation with various thickness ratios ($\beta_w=0.1$; $\beta_s=0.02$)

5. Results and discussion

In this section, numerical results of bending, buckling and vibrations behaviors of CNTRC beams are presented and discussed. The effective material characteristics of CNTRC beams at ambient temperature employed throughout this work are given as follows. Poly methyl methacrylate (PMMA) is utilized as the matrix and its material properties are: $\nu^p = 0.3$ and $E^p = 2.5GPa$. For reinforcement material, the armchair (10,10) SWCNTs is chosen with the following properties (Tagrara 2015, Yas and Samadi 2012): $\nu_{11}^{cnt} = 0.19$; $E_{11}^{cnt} = 600GPa$; $E_{22}^{cnt} = 10GPa$ and $G_{12}^{cnt} = 17.2GPa$.

For convenience, the following nondimensionalizations are employed

$$\bar{N} = \frac{N_x^0}{A_{110}} \quad (19)$$

5.1 Results for buckling analysis of CNTRC beams

Table 1 Comparison of critical loads for CNTRC beam with and without elastic foundation ($L/h=15$, $V_{cnt}^* = 0.12$)

| Source | $\beta_w=0, \beta_s=0$ | | | $\beta_w=0.1, \beta_s=0.02$ | | |
|--|------------------------|---------|--------|-----------------------------|--------|--------|
| | UD | O | X | UD | O | X |
| FSDBT ^(a) ($\epsilon_z=0$) | 0.1032 | 0.0604 | 0.1367 | 0.1333 | 0.0905 | 0.1668 |
| TSDBT ^(a) ($\epsilon_z=0$) | 0.0985 | 0.0575 | 0.1291 | 0.1287 | 0.0876 | 0.1590 |
| Ref ^(b) ($\epsilon_z=0$) | 0.0986 | 0.0588 | 0.1288 | 0.1287 | 0.0889 | 0.1590 |
| Tagrara ^(c) ($\epsilon_z=0$) | 0.0985 | 0.0575 | 0.1291 | 0.1286 | 0.0876 | 0.1592 |
| Present ($\epsilon_z=0$) | 0.09266 | 0.05356 | 0.1226 | 0.1227 | 0.0836 | 0.1527 |

(a) Taken from Wattanasakulpong and Ungbhakorn (2013)

(b) Taken from Yas and Samadi (2012)

(c) Taken from Tagrara (2015)

In this section, numerical results of buckling analysis of CNTRC beams are discussed. The present theory with stretching effect ($\epsilon_z \neq 0$) are compared with the analytical solutions given by Wattanasakulpong and Ungbhakorn (2013) using third shear deformation CNTRC beam theory and Timoshenko CNTRC beams documented by Wattanasakulpong and Ungbhakorn (2013) and Yas and Samadi (2012), and the results of Tagrara *et al.* (2015) as shown in Table 1. It can be observed that our results with ($\epsilon_z \neq 0$) are in an excellent agreement to those predicted using the higher order shear deformation theory of Wattanasakulpong and Ungbhakorn (2013), Yas and Samadi (2012) and Tagrara *et al.* (2015) with ($\epsilon_z \neq 0$) respectively. However, the small difference found between the results is due to that the theories presented by Wattanasakulpong *et al.* (2013), Yas and Samadi (2012) and Tagrara *et al.* (2015) ignore the thickness stretching effect. The X-Beam is the strongest beam that supports the largest buckling load and followed by the UD-Beam and O-Beam.

Figs. 2 and 3 show respectively the influence of both Winkler modulus parameter and the Pasternak shear modulus on the buckling load with stretching effect ($\epsilon_z \neq 0$) of different types of CNTRC beams. It is observed that the buckling loads increase linearly as the increase of the spring constant factors.

The effect of volume fractions of CNTs on the critical buckling load of the strongest beam (X-beam) is shown in Fig. 4 using the present trigonometric refined beam theory with stretching effect ($\epsilon_z \neq 0$). Decreasing the volume fractions of CNTs leads to reduction in the buckling loads. The dramatic reduction of the buckling loads is observed in the range of $L/h=10$ to 30.

6. Conclusions

In this present study, a refined shear deformation beam theory with stretching effect is employed to investigate the buckling problem of simply supported CNTRC beams resting on elastic foundation. The beams are reinforced by different patterns of CNT distributions in the polymeric matrix. The equilibrium equations have been obtained using

the principle of virtual displacements. The accuracy of the mathematical models is numerically verified by comparison with some available results. From the numerical results, it is found that the X-Beam is the strongest among different types of CNTRC beams in supporting the buckling, while the O-Beam is the weakest.

References

- Barzoki, A.A.M., Loghman, A. and Ali Ghorbanpour Arani, A.G. (2015), "Temperature-dependent nonlocal nonlinear buckling analysis of functionally graded SWCNT-reinforced microplates embedded in an orthotropic elastomeric medium", *Struct. Eng. Mech.*, **53**(3), 497-517.
- Berrabah, H.M., Tounsi, A., Semmah, A and Adda Bedia, E.A. (2013), "Comparison of various refined nonlocal beam theories for bending, vibration and buckling analysis of nanobeams", *Struct. Eng. Mech.*, **48**(3), 351-365.
- Bourada, M., Kaci, A., Houari, M.S.A. and Tounsi, A. (2015), "A new simple shear and normal deformations theory for functionally graded beams", *Steel Compos. Struct.*, **18**(2), 409-423.
- Coleman, J.N., Khan, U., Blau, W.J. and Gunko, Y.K. (2006), "Small but strong: A review of the mechanical properties of carbon nanotube-polymer composites", *Carbon*, **44**(9), 1624-1652.
- Draiche, K., Tounsi, A. and Mahmoud, S.R. (2016), "A refined theory with stretching effect for the flexure analysis of laminated composite plates", *Geomech. Eng.*, **11**(5), 671-690.
- Hajnayeb, A. and Khadem, S.E. (2015), "An analytical study on the nonlinear vibration of a doublewalled carbon nanotube", *Struct. Eng. Mech.*, **54**(5), 987-998.
- Hamidi, A., Houari, M.S.A., Mahmoud, S.R. and Tounsi, A. (2015), "A sinusoidal plate theory with 5-unknowns and stretching effect for thermomechanical bending of functionally graded sandwich plates", *Steel Compos. Struct.*, **18**(1), 235-253.
- He, X.Q., Rafiee, M. and Mareishi, S. (2015), "Nonlinear dynamics of piezoelectric nanocomposite energy harvesters under parametric resonance", *Nonlin. Dyn.*, **79**(3), 1863-1880.
- Hu, N., Fukunaga, H., Lu, C., Kameyama, M. and Yan, B. (2005), "Prediction of elastic properties of carbon nanotube reinforced composites", *P. Roy. Soc. A*, **461**(2058), 1685-1710.
- Ke, L.L., Yang, J. and Kitipornchai, S. (2013), "Dynamic stability of functionally graded carbon nanotube-reinforced composite beams", *Mech. Adv. Mater. Struct.*, **20**(1), 28-37.
- Lei, Z.X., Liew, K.M. and Yu, J.L. (2013), "Large deflection analysis of functionally graded carbon nanotube-reinforced composite plates by the element-free kp-ritz method", *Comput. Meth. Appl. Mech. Eng.*, **256**, 189-199.
- Mareishi, S., Rafiee, M. He, X.Q. and Liew, K.M. (2014), "Nonlinear free vibration, postbuckling and nonlinear static deflection of piezoelectric fiber-reinforced laminated composite beams", *Compos. Part B: Eng.*, **59**, 123-132.
- Rafiee, M., He, X.Q. and Liew, K.M. (2014), "Non-linear dynamic stability of piezoelectric functionally graded carbon nanotube-reinforced composite plates with initial geometric imperfection", *Int. J. Non-Linear Mech.*, **59**, 37-51.
- Rafiee, M., He, X.Q., Mareishi, S. and Liew, K.M. (2015), "Nonlinear response of piezoelectric nanocomposite plates: Large deflection, post-buckling and large amplitude vibration", *Int. J. Appl. Mech.*, **7**(5), 1550074.
- Rafiee, M., Mareishi, S. and Mohammadi, M. (2012), "An investigation on primary resonance phenomena of elastic medium based carbon nanotubes", *Mech. Res. Commun.*, **44**(1), 51-56.
- Rafiee, M., Nitzsche, F. and Labrosse, M. (2017), "Dynamics, vibration and control of rotating composite beams and blades: A critical review", *Thin-Wall. Struct.*, **119**, 795-819.
- Rafiee, M., Yang, J. and Kitipornchai, S. (2013), "Thermal bifurcation buckling of piezoelectric carbon nanotube reinforced composite beams", *Comput. Math. Appl.*, **66**(7), 1147-1160.
- Ray, M.C. and Batra, R.C. (2007), "A single-walled carbon nanotube reinforced 1-3 piezoelectric composite for active control of smart structures", *Smart Mater. Struct.*, **16**(5), 1936-1947.
- Tagrara, S.H., Benachour, A., Bachir Bouiadja, M. and Tounsi, A. (2015), "On bending, buckling and vibration responses of functionally graded carbon nanotube-reinforced composite beams", *Steel Compos. Struct.*, **19**(5), 1259-1277.
- Wattanasakulpong, N. and Ungbhakorn, V. (2013), "Analytical solutions for bending, buckling and vibration responses of carbon nanotube-reinforced composite beams resting on elastic foundation", *Comput. Mater. Sci.*, **71**, 201-208.
- Yas, M.H. and Samadi, N. (2012), "Free vibrations and buckling analysis of carbon nanotube-reinforced composite Timoshenko beams on elastic foundation", *Int. J. Pres. Vess. Pip.*, **98**, 119-128.
- Zhu, R., Pan, E. and Roy, A.K. (2007), "Molecular dynamics study of the stress-strain behavior of carbon-nanotube reinforced Epon 862 composites", *Mater. Sci. Eng. A.*, **447**(1-2), 51-57.

CC